Journal of Orthopaedic Translation (2019) 19, 47—57

Available online at www.sciencedirect.com

ScienceDirect

journal homepage: http://ees.elsevier.com/jot

ORIGINAL ARTICLE

Andrographolide stimulates osteoblastogenesis and bone formation by inhibiting nuclear factor kappa-B signaling both *in vivo* and *in vitro*

Chang Yongyun ☆, **Zhang Jingwei** ☆, **Liu Zhiqing, Chu Wenxiang, Li Huiwu***

Shanghai Key Laboratory of Orthopaedic Implants, Department of Orthopaedics, Shanghai Ninth People's Hospital, Shanghai Jiao Tong University School of Medicine, Shanghai 200011, People's Republic of China

Received 11 November 2018; received in revised form 23 January 2019; accepted 7 February 2019
Available online 2 March 2019

KEYWORDS
Andrographolide;
NF-kB;
Osteoblast;
Osteoporosis;
TNF-α

Abstract Osteoporosis is a bone disease that is associated with a decrease in bone mineral density, deterioration of bone microarchitecture and increased fracture risk. Currently, available treatments mainly focus on either inhibiting osteoclast function, such as administration of bisphosphonate, calcitonin, oestrogen, selective oestrogen receptor modulator and so on, or stimulating osteoblasts, such as parathyroid hormone, to improve bone mass and skeletal microarchitecture. However, there is no option that is completely satisfactory because of the limitations of monotherapy with either class. Thus, it is highly appealing to investigate novel drugs with both antiresorptive and osteoanabolic activities that have the potential to be more beneficial than monotherapy because of the different mechanism of action. As has been proven in previous study that andrographolide (AP), as a key herbal medicine, could suppress osteoclast formation and function both in vivo and *in vitro*. The purpose of this present study was to identify the effect of AP on osteoblast differentiation and oestrogen deficiency —induced osteoporosis. It was concluded that AP significantly reduced oestrogen deficiency —induced bone loss in vivo. Furthermore, it was proved that tumor necrosis factor alpha severely impaired bone morphogenetic protein-2 (BMP-2)—induced osteoblast differentiation, and this inhibition could be greatly attenuated by AP. This was further supported by the fact that AP significantly increases the expression of osteoblast-specific markers, including runt-related transcription factor-2, osteocalcin and osteopontin. In addition, molecular analysis revealed that AP greatly ceased tumor necrosis factor alpha—mediated stimulation of nuclear factor kappa-B activity, whereas overexpression of the nuclear factor kappa-B subunit p65

* Corresponding author. Zhizaoju Road, Shanghai 200011, China. Tel./fax: +86 21 63139920639.
E-mail address: huiwu1223@163.com (L. Huiwu).
☆ These authors contributed equally to this work.

https://doi.org/10.1016/j.jot.2019.02.001

reversed the stimulatory effects of AP on osteoblast differentiation. Thus, combined with previous study, AP was demonstrated to be a novel agent with both antiresorptive and osteoanabolic activities and had the potential to be developed as an antiosteoporosis alternative.
The translational potential of this article: This study provides strong evidence for the identification that AP has both antiresorptive and osteoanabolic activities and thus has great potential to be developed as a novel antiosteoporosis agent.

Introduction

Bone is a kind of organ which is rigid but dynamic, and it is shaped and maintained continuously. A balance between delicate osteoblastic bone formation and resorption can repair the strength and integrity of bone. However, if the rate of bone resorption is higher than that of bone formation, it will cause adult skeletal diseases, including osteoporosis. In particular, with increased longevity and unhealthy lifestyles, osteoporosis, a skeletal disorder which features reduced bone mineral density, deteriorated bone microarchitecture and higher fractures risk (particularly in the hip), is a major concern. This could create severe issues, such as substantial skeletal deformity, pain and functional limitation, and could enhance mortality, which is a serious burden for the economy (NIH Consensus, 2001).

To prevent and treat osteoporosis, antiresorptive drugs are still the cornerstone of therapy [1—4]. However, current antiresorptive drugs, although useful, are not completely satisfactory, in general, because they are not related to theatrical growth in bone mass. The coordination of anabolic and antiresorptive treatment may be required for the optimal treatment of osteoporosis. Through the stimulation of bone formation, based on bone quality improvement and bone mass increase, fracture incidence may be reduced by anabolic agents. At present, there is only one anabolic agent with approval from the US Food and Drug Administration, that is, recombinant human parathyroid hormone (PTH); however, its effect is greatly attenuated without the continuous use of antiresorptive drugs [5—7]. Moreover, PTH cannot be administered to patients who have osteosarcoma. In addition, there is distrust in its use as several observational studies do not fully support the combination of two drugs in the same class [8,9]. Romosozumab, a monoclonal antibody targeting sclerostin, can increase trabecular and cortical bone volume and strength through promoting bone formation and reducing bone resorption simultaneously. However, studies have shown that the bone-forming effects of romosozumab are attenuated over time, whereas its antiresorptive effects persist [10]. It is also reported that the number of adjudicated severe cardiovascular events is higher in the romosozumab group than in the alendronate group [11]. Based on the aforementioned analysis, it is imperative to develop new drugs with both anabolic and antiresorptive functions.

Historically, natural compounds and their derivatives were deemed priceless because they are a source of therapeutic agents. Many natural compounds have positive effects on the skeleton because of their counteractive effect [12—14]. As a key herbal plant from which medicine is derived, *Andrographis paniculata* is widely used in Southeast Asian countries. It is widely used in the clinic for fever treatment, inflammation, diarrhoea and other infectious diseases without any obvious side effects [15—17]. *A. paniculata* is one of the main sources of diterpene lactones, and andrographolide (AP) is one of the factors that contain 70% of the plant extract [18]. It was shown in many studies that AP has antiinflammatory, anticancer and hepatoprotective activities by acting in different signaling pathways such as nuclear factor kappa-B (NF-κB) and p38 phosphatidyl inositol 3-kinase/Akt pathways [19—23]. In previous study, through attenuating the NF-κB signaling pathway, it was shown that osteoclast formation and function are suppressed by AP. The aim of this article is to determine the influences of AP on the differentiation of osteoblasts and bone formation in rats. Considering fragile fractures, we investigated the influences of AP on vertebral biomechanical features in ovariectomized rats.

Materials and methodologies

Media and reagents

AP was bought from Sigma-Aldrich (USA), and Alpha minimum Eagle's medium (Alpha-MEM), foetal bovine serum and penicillin were bought from Gibco BRL (Gaithersburg, MD, USA). However, the CCK-8 assay kit was bought from Dojindo Molecular Technology (Japan). Tumor necrosis factor alpha (TNF-α) and BMP-2 were bought from R&D Systems (USA).

Rat ovariectomy surgery and bone formation assay

The animal experimental and surgical procedure were carried out in the Animal Laboratory, Shanghai Ninth Hospital, Shanghai Jiao Tong University School of Medicine, Shanghai, China. National guidelines for the care and use of laboratory animals have been observed. The animal experimental protocols was approved by Shanghai Ninth Hospital, Shanghai Jiao Tong University School of Medicine, Animal experimental ethic Committee. Forty-eight female Sprague—Dawley rats aged 24 months, bought from Sino-British Sippr/BK Lab Animal Ltd, Shanghai, in China, were equally classified into three groups: (1) sham; (2)

ovariectomy (OVX) and (3) ovariectomy plus AP (OVX + AP) (50 mg/kg/day) [24–26]. One month after surgery, AP was administered orally once a day for 60 days. Tetracycline, alizarin red and calcein were injected subcutaneously for bone labelling 15, 7 and 2 days before sacrifice to obtain a fluorescent label at the sites of active bone-forming surfaces. At sacrifice, we collected samples of blood and bone. Then, the fourth lumbar vertebra (L4) was dissected for analysis by microcomputed tomography (micro-CT) and histomorphometry in sequence (with four sample reduplications), along with biomechanical testing. Meanwhile, L4 was fixed in 4% paraformaldehyde (PFA) and embedded in methyl methacrylate (with four sample reduplications). Unstained transverse sections were examined with a fluorescent microscope. Mineral appositional rate (MAR) and bone-formation rate were measured using the OsteoMeasureXP Software (OsteoMetrics, Inc., GA, USA) (with four sample reduplications).

Micro-CT and histomorphometry analysis

We scanned L4 with a high-resolution micro-CT scanner (Skyscan 1072; Skyscan, Aartselaar, Belgium), as previously described [27]. We measured the microstructural indices of trabecular bone density (BV/TV), trabecular thickness (Tb.Th), trabecular number (Tb.N) and trabecular space (Tb.Sp). For histological examination, we fixed L4 in 70% ethanol and stained with hematoxylin and eosin (H&E). Four samples in each group were analysed for reduplication.

Biomechanical testing

To subject the vertebra to three-point bending and axial compression, we used a servohydraulic testing machine (MTS 858 Mini Bionix II; MTS Systems Corp., Minneapolis, MN, USA). L4 was subjected to compression at a displacement rate of 6 mm/min. We used TestStar II Electric-hydraulic Servo Universal Test software (MTS Systems Corporation, MN, USA) to conduct the analysis of the load–deformation curves. By following the fracture of the specimen, we measured and recorded the force and displacement data. The following biomechanical parameters were confirmed by the load–deformation curve, including maximum load (N; the load at the maximum failure point) and Young's modulus (GPa; maximum slope of the stress–strain curve). Four samples in each group were analysed for reduplication.

Serum osteocalcin and P1NP

Serum osteocalcin and P1NP were measured using an ELISA MK127 kit (Takara Shuzo, Kyoto, Japan) based on the instructions of the manufacturer. There were 12 samples in each group for reduplication.

Primary cell isolation and culture

The femurs of the rats were incubated in complete culture media for proliferation, from which bone marrow stromal cells (BMSCs) were extracted. When confluence reached 90%, we used phosphate-buffered saline to wash cells and for trypsinization to harvest BMSCs.

Fluorescence-activated cell sorting

The BMSCs taken from the rats were layered onto a lymphocyte-M gradient (Cedarlane Laboratories, Burlington, Ontario, Canada). We collected and incubated the cells with allophycocyanin-conjugated anti-CD140a for 30 min. We cleaned the cells twice and conducted the analysis based on the Cytomics FC500 (Beckman Coulter, Fullerton, CA, USA).

Cytotoxicity assay

The influence of AP proliferation was determined with a Cell Counting Kit-8 (CCK-8; Dojindo Molecular Technology) based on the instructions of the manufacturer. The primary BMSCs were plated in 96-well plates with the density of 5×10^3 cells/well with three replications. We used increasing concentrations of AP to treat the cells 24 h later (0, 2, 10, and 20 μM) for 2 days. Then, we added 10 μl of CCK-8 in each well and incubated these plates at 37 °C for 2 h. Through an ELX800 absorbance microplate reader (Bio-Tek, USA), which had a wavelength of 450 nm (650 nm reference), optical density was measured.

Alizarin red S staining

During the late period of osteogenic differentiation, calcium deposition was examined by alizarin red S staining, following the manufacturer's instructions. In brief, we used cold phosphate-buffered saline to clean the cultured cells, fixed the cells for 15 min in 4% PFA and stained with 0.2% alizarin red S solution (Sigma-Aldrich) for 30 min. To remove nonspecific precipitation, we used deionized water to clean the stained cells thoroughly. Calcium deposits on the differentiated cells were represented by positive red staining.

Quantitative polymerase chain reaction analysis

Each well was seeded with BMSCs in 24-well plates with the density of 1×10^6 cells with three replications. Using an RNeasy Mini kit (Qiagen, Valencia, CA, USA), total RNA was prepared based on the instructions of the manufacturer. In addition, reverse transcription reaction(TaKaRa Biotechnology) was performed, and we synthesized cDNA from 1 μg of total RNA. Real-time PCR was performed using the SYBR Premix Ex Tag kit (TaKaRa Biotechnology, Beijing, China) in an ABI 7500 (http://www.takara.com.cn) Sequencing Detection System. The following PCR conditions were programmed with the detector: 40 cycles for 5 s denaturation at 95 °C and 34 s amplification at 60 °C. In the end, each reaction was run in triplicates for the normalization of the housekeeping gene β-actin. Primer sequences were as follows: β-actin 5′-TCTGCTGGAAGGTGGACAGT-3′ (forward) and 5′-CTGGGT CATCTTTTCACGGT-3′ (reverse), runt-related transcription factor-2 (Runx2) 5′-TCCTGTAGATCCGAGCACCA-3′ (forward) and 5′-CTGCTGCTGTTGTTGCTGTT-3′ (reverse), osteopontin

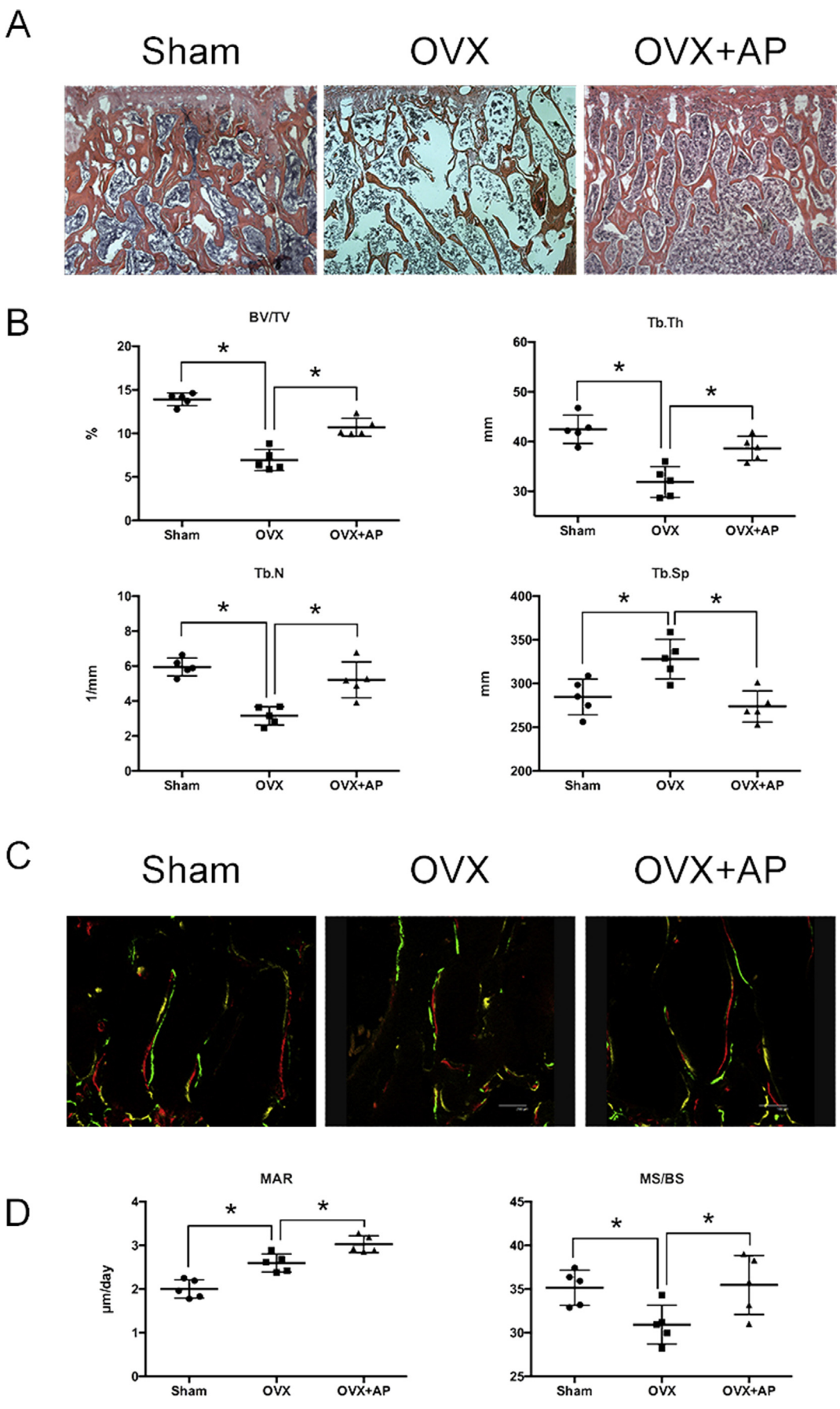
A
Sham
OVX
OVX+AP
B
BV/TV
%
Tb.Th
mm
Tb.N
1/mm
Tb.Sp
mm
Sham
OVX
OVX+AP
C
Sham
OVX
OVX+AP
D
MAR
μm/day
MS/BS
Sham
OVX
OVX+AP

(OPN) 5′-TGTTCCTACCAAGATTATACCAAAT-3′ (forward) and 5′-CGCTCGATTTGCAGGTCTTT-3′ (reverse), and osteocalcin (OCN) 5′-AAGCAGGAGGGCAATAAGGT-3′(forward) and 5′-TTTGTAGGCGGTCTTCAAGC-3′ (reverse).

Plasmid transfer and luciferase assay

The BMSCs were transfected with pGL4.32 [luc2P/NF-κB-RE/Hygro] vector to determine NF-κB activity. pRL Renilla luciferase control vector, Promega, WI, USA was also used to transform cells into BMSCs using pGL4.32 [luc2P/NF-κB-RE/Hygro] vector as insider management. Two plasmids were purchased from Promega Corp., Promega, WI, USA and transfected into cells with Lipofectamine® 2000 (Invitrogen Life Technologies, CA, USA). The cells were seeded at 0.5×10^5 cells/well in a 24-well plate and were activated using 200 ng/ml of BMP-2, 10 ng/ml of TNF-α and/or AP, 24 h after plasmid transformation. The cells were grown at 37 °C and collected after 48 h. A double luciferase reporter system (Promega Corp.) was used to estimate luciferase activity.

Cell spreading assay

Through detection of filamentous actin of the cytoskeleton of BMSCs, we investigated cell spreading. We incubated the cells on titanium plates for 24 h. The cells were fixed with 4% paraformaldehyde and permeabilized with Triton X-100 (0.1%). Then, cells were stained with rhodamine phalloidin (5 units•mL-1; Biotium, Hayward, CA, USA) for 30 min. We visualized the cytoskeleton by confocal laser scanning microscopy using a Leica Microsystems TCS SP2 (Heidelberg, Germany).

Statistical analysis

Statistical significance was determined by the Student t test. A p-value less than 0.05 was considered statistically significant.

Results

AP prevented bone loss and increased new bone formation in ovariectomized rats

As shown in Fig. 1A, histological tests of L4 models demonstrated an obvious recovery of the trabecular structure in the ovariectomized rats with AP treatment. This was consistent with the microstructural indices of trabecular bone density (BV/TV), trabecular thickness (Tb.Th), trabecular number (Tb.N) and trabecular space (Tb.Sp) in micro-CT image analysis (Fig. 1B). To further confirm whether AP stimulated new bone formation, AP (50 mg/kg per day) was administered orally followed by tetracycline, alizarin red and calcein labelling, and the analysis of histomorphometric parameters indicated obvious differences between the groups, indicated by increasing MAR and MS/BS. (Fig. 1C and D).

Then, to evaluate the effects of AP on BMSCs maintenance, the BMSCs from the rats of the OVX or OVX + AP groups were examined via flow cytometry analysis. There were significantly more BMSCs positive for markers such as CD140a [28] in the AP group (Fig. 2A). These results indicate that AP administration increases BMSCs distribution. To further examine the effects of AP on BMSCs, the cells isolated from the sham, OVX and OVX + AP groups were cultured in osteoblast differentiation medium for 2 weeks. Alizarin red S staining indicated that the area of calcium nodules was significantly higher in the OVX + AP group than that in the sham and OVX groups (Fig. 2B and C). It was shown that the population of osteoblast precursor cells increased in AP-treated rats. To evaluate bone formation activity, serum levels of P1NP and osteocalcin, which are bone formation markers, were estimated by enzyme-linked immunosorbent assay (ELISA). As shown in Fig. 2D, both P1NP and osteocalcin levels were higher in the OVX + AP group than those in the sham group. These results indicate that AP stimulated bone formation in OVX rats.

AP improved biomechanical properties of bone

With respect to deciding whether AP can improve bone biomechanical properties or not, we used an *ex vivo* axial compression test for the examination of biomechanical competence of the lumbar vertebral bodies. When Young's modulus was compared with the sham group, there was a theatrical drop in the lumbar vertebrae after OVX, which can be significantly improved by AP treatment. In addition, AP helped to rescue the maximum load decrease due to OVX (Fig. 2E).

AP stimulated osteoblast differentiation and cell spreading *in vitro*

First, we excluded the possibility of cell cytotoxicity of AP using proliferation analysis (Fig. 3A and B). To study AP's influence on osteoblastogenesis, we treated the BMSCs with osteoblast-inducing conditional media and indicated doses of AP during the course of osteoblast differentiation. After 2 weeks of culture after treatment with AP, we performed alizarin red staining and demonstrated that AP enhanced calcium nodule formation (Fig. 3C and D). These results were further confirmed by the upregulation of marker genes of osteoblast differentiation, such as Runx2, osteocalcin (OCN) and OPN (Fig. 3E). Fig. 3F shows that confocal

Figure 1 AP treatment increases bone formation in lumbar vertebrae as assessed by histomorphometric analysis. (A) H&E staining of lumbar vertebra. (B) Micro-CT analyses of the lumbar vertebra, bone volume per tissue volume (BV/TV) ratio, trabecular thickness (Tb.Th), trabecular number (Tb.N) and trabecular separation (Tb.Sp). (C) Fluorescent micrograph of the trabecular bone section showing tetracycline (yellow), alizarin red (red) and calcein (green) labels. (D) MAR and MS/BS. Data are presented as mean ± SD; *P < 0.05. AP, andrographolide; MAR, mineral appositional rate; Micro-CT, microcomputed tomography; OVX, ovariectomy; OVX + AP, ovariectomy plus andrographolide; SD, standard deviation ; H&E, hematoxylin and eosin, MS/BS, bone mineralising surface

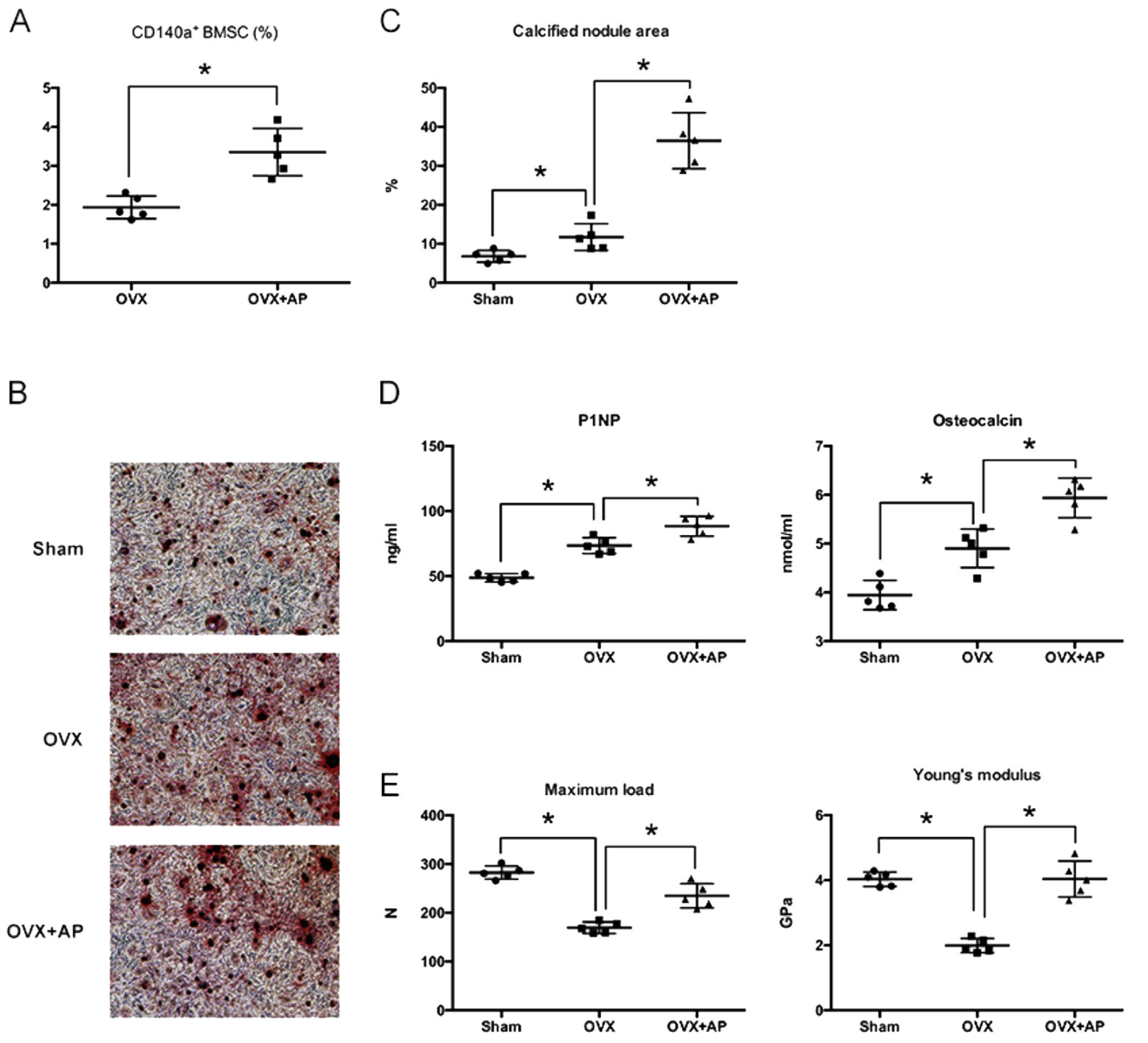

Figure 2 AP stimulates osteoblast mineralization *ex vivo* and improves biomechanical properties of lumbar vertebrae. (A) Quantification of CD140a^{+} cells in the bone marrow cells isolated from indicated rats 1 week after OVX. (B) Representative images of alizarin red staining of BMSCs isolated from the indicated rats. (C) Quantification of mineralized nodules of BMSCs isolated from the indicated rats. (D) Serum P1NP and osteocalcin levels. (E) Vertebral maximum load (N) and Young's modulus (GPa). Data are presented as mean $\pm$ SD; *P $<$ 0.05. AP, andrographolide; BMSCs, bone marrow stromal cells; OVX, ovariectomy; OVX + AP, ovariectomy plus andrographolide; SD, standard deviation.

laser scanning microscopy can be used to observe the cytoskeleton of BMSCs after 24 h of culture. The cells in AP treatment showed clustering, confluence and multilayer morphology with more actin filaments linking to adjacent cells, but the cells in the control appeared dispersive, had a monolayer and were reduced in number (Fig. 3G).

AP blocked TNF-α—mediated suppression of osteoblast differentiation

It has been shown in the previous research that the influence of TNF-α—induced NF-κB activation on bone creation is antianabolic in differentiating osteoblasts [29]. In the final period of osteoblast differentiation, features are formed based on creating mineral extracellular matrix. Therefore, AP's influence on the late period of osteoblast differentiation in the presence of TNF-α requires further study. Based on the study by alizarin red S staining, differentiation of BMP-2—stimulated osteoblasts is impaired by TNF-α in a significant way, and this trend was ceased by the addition of AP (Fig. 4A). The same trend was identified by subsequent calcified nodule quantification, which showed that differentiation of TNF-α—mediated suppression of late-stage osteoblasts can be blocked by AP (Fig. 4B and C).

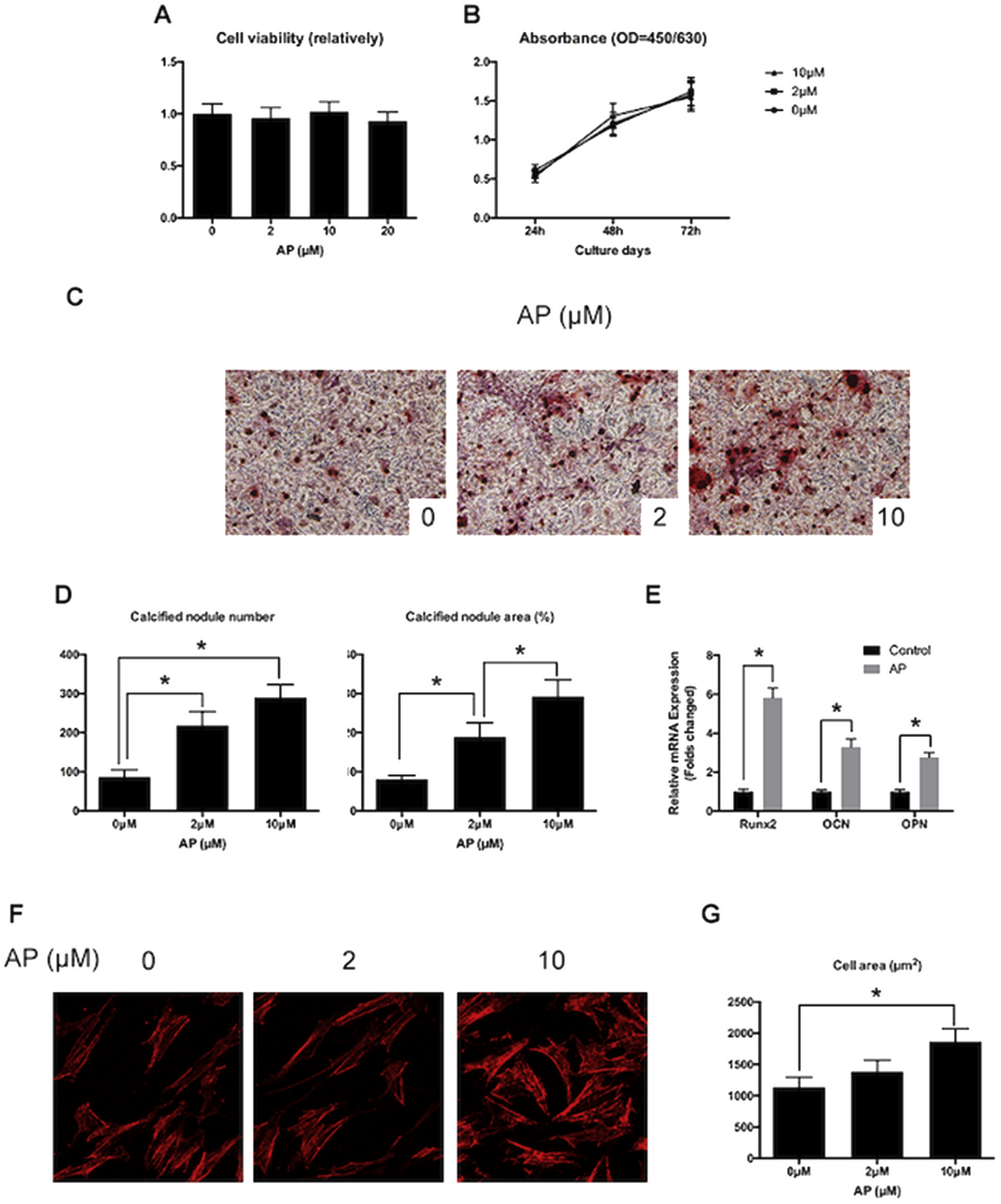

Figure 3 AP stimulates osteoblast differentiation and mineralization dose-dependently without causing cytotoxicity *in vitro*. (A) BMSCs were treated with the indicated concentrations of AP for 48 h, and cell growth was estimated using the CCK-8 assay. (B) BMSCs were treated with the indicated concentrations of AP for the specified days, and cell growth was estimated using the CCK-8 assay. (C) On Day 14, the cells were subjected to alizarin red S staining. (D) The number of calcified nodules analysed. (E) mRNA expression of OCN, OPN and Runx2. (F) Confocal laser scanning microscope. (G) Cell spreading area. Data are presented as mean $\pm$ SD; *P $<$ 0.05. AP, andrographolide; BMSCs, bone marrow stromal cells; CCK-8, Cell Counting Kit-8; OCN, osteocalcin; OPN, osteopontin; Runx2, runt-related transcription factor-2; SD, standard deviation; OD, Optical density

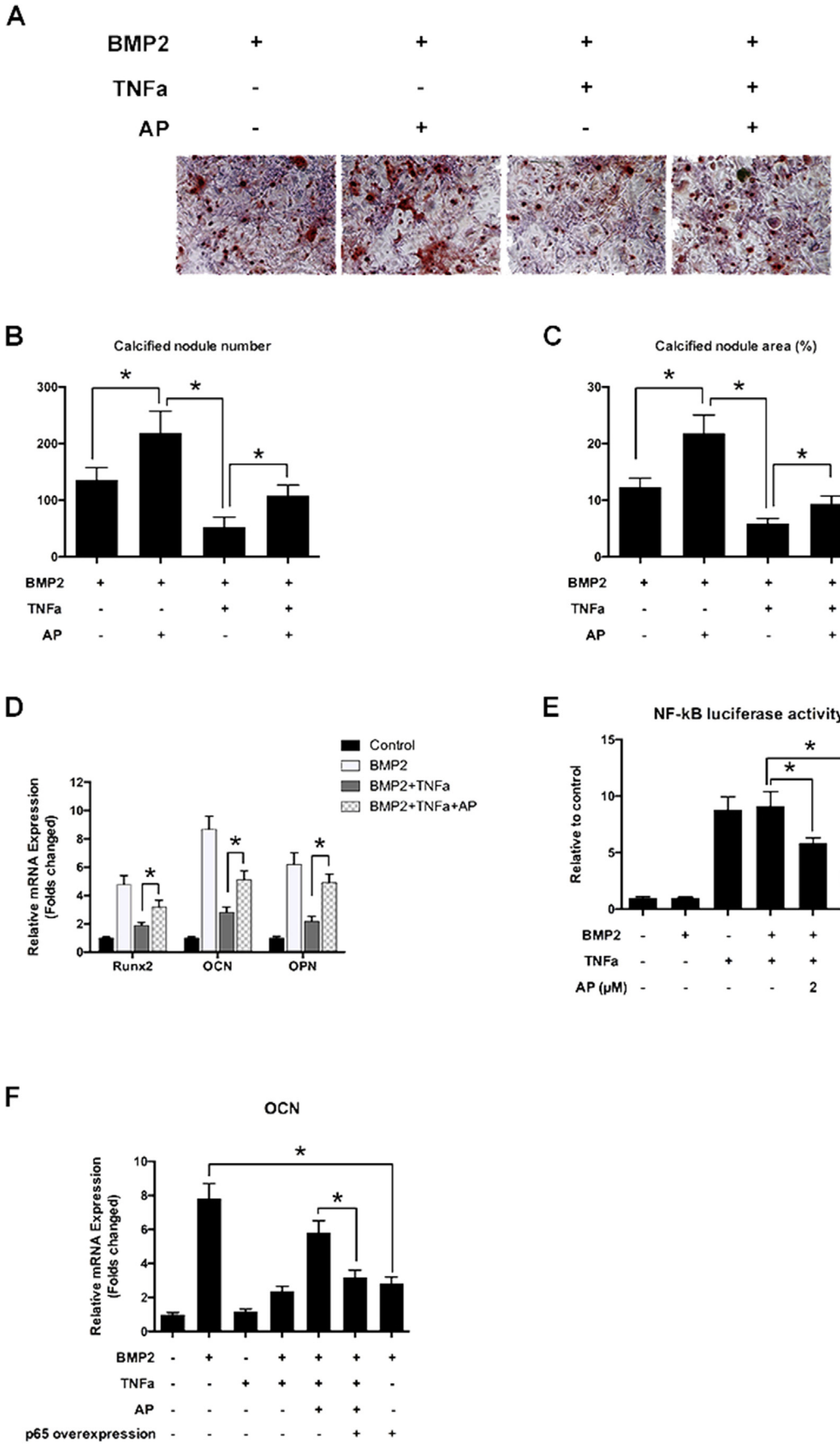
A
BMP2 + + + +
TNFa - - + +
AP - + - +
B
Calcified nodule number
300
200
100
0
BMP2 + + + +
TNFa - - + +
AP - + - +
C
Calcified nodule area (%)
30
20
10
0
BMP2 + + + +
TNFa - - + +
AP - + - +
D
Control
BMP2
BMP2+TNFa
BMP2+TNFa+AP
Relative mRNA Expression (Folds changed)
12
10
8
6
4
2
0
Runx2
OCN
OPN
E
NF-kB luciferase activity
Relative to control
15
10
5
0
BMP2 - + - + + +
TNFa - - + + + +
AP (μM) - - - - 2 10
F
OCN
Relative mRNA Expression (Folds changed)
10
8
6
4
2
0
BMP2 - + - + + + +
TNFa - - + + + + -
AP - - - - + + -
p65 overexpression - - - - - + +

AP downregulated TNF-α—mediated stimulation of NF-κB activity

It was found that NF-κB signaling played an important role in osteoblast differentiation. Particularly, it inhibits osteoblast differentiation by interfering with Smad activity downstream of BMP-2 or transforming growth factor-β (TGFβ) [30]. Similarly, osteoblast differentiation and BMP-2 responsiveness could be increased by blocking NF-κB [31]. To determine the mechanism through which AP may affect osteoblast differentiation, the influence of AP on NF-κB signaling was investigated. The function of AP in TNF-α—induced NF-κB activity inhibition was estimated by the luciferase assay (Fig. 4E). It was shown that NF-κB luciferase activity increases in osteoblasts after TNF-α treatment. Luciferase activity stimulation was significantly weakened by AP, which shows that NF-κB activation and suppression is affected in a dose-dependent manner. It was also shown that, in osteoblasts, NF-κB signaling is suppressed by AP. In addition, to prove whether osteoblast differentiation is affected by the rescue of NF-κB activity or not, the expression of osteoblast-specific genes was estimated (Fig. 4D). AP seemed to keep the expression of the OCN gene in a significant way, which agrees with the previous conclusions. However, AP could help to rescue the expression of OCN in an efficient way when cells are overexpressing p65 (Fig. 4F). All aforementioned studies show that AP mechanism of action in the differentiation of osteoblasts contains NF-κB stimulation and inhibition.

Discussion

In the current research, the influence of AP on osteoblast differentiation and function in rats were investigated. *In vivo* results demonstrated that AP stimulated new bone formation and enhanced bone mechanical strength. Moreover, it was found that AP promoted differentiation of osteoblasts and mineralization *in vitro*, which was further supported by the upregulation of osteoblast-specific gene markers such as Runx2, OCN and OPN in a dose-dependent manner. In addition, AP was found to significantly prevent TNF-α—induced suppression of osteoblast formation and mineralisation. By studying the expression of Runx2, it was proven that AP protected against TNF-α—induced suppression from the expression of osteoblast marker genes, which concluded that through inhibitory action of TNF-α prevention, osteoblast differentiation is restored by AP, which improves the expression of osteogenic-specific genes, alkaline phosphatase (ALP), OCN and OPN, in a dose-dependent manner. The function of AP on the expression of genes requires further study. BMP-2 has significant upregulation expression of osteoblast-specific genes compared with the negative control, but this influence will disappear when TNF-α appears. The additional AP is totally different from TNF-α—induced suppression of osteoblast gene expression in an effective manner, which indicates the AP's ability to block the osteoblastogenesis suppression at the level of transcription. Further studies are also needed to ascertain whether the influence of AP on osteoblast differentiation can be expressed by NF-κB activation suppression. The luciferase assay results allowed us to conclude that AP treatment suppressed NF-κB activation. In the meantime, AP-induced osteoblastogenesis was stopped by the overexpression of NF-κB subunit p65, which confirms that AP adjusted the differentiation of osteoblasts through NF-κB suppression. This observation was further supported by analysing osteoblast gene expression.

Recently, several studies have shown that the NF-κB pathway played an important role in regulation of osteoblast differentiation. Activation of NF-κB signaling decreased osteogenesis of mesenchymal stem cells. Initially, Jimi et al. [30] and Gilbert et al. [32] described that inflammation, especially TNF-α, could inhibit osteoblast differentiation through NF-κB signaling. Li et al. [33] demonstrated that TNF-α suppressed BMP-2 and mediated Smad activation by induction of NF-κB and overexpression of p65/p50 which mimicked TNF-α effects. Consistently, they also claimed that NF-κB pharmacological suppression augmented osteoblast differentiation and mineralization *in vitro*. Chang et al. [34]and Lin et al. [35] revealed that NF-κB activation was highly correlated with inflammation-associated bone diseases. Targeting NF-κB activity in mesenchymal stem cells (MSCs) had the potential to modulate bone loss or enhance bone regeneration and repair. Furthermore, Wang et al. [36] showed that NF-κB signaling played important roles in regulation of bone remodeling and that TNF receptor associated factor (TRAF) family members were vital mediators in NF-κB signaling. Carboxyl terminus of Hsp70-interacting protein functioned as a critical regulator in NF-κB signaling through regulation of multiple TRAF family members in osteoblast differentiation. Our study supports these results in BMSCs as blocking NF-κB showed increased osteoblast differentiation and BMP-2 responsiveness.

In summary, our study shows that the formation of new bone and prevention of bone loss caused by oestrogen deficiency can be induced by AP, thus improving bone quality and biomechanical properties. These in vivo effects were achieved by stimulating osteoblast differentiation and mineralization. AP may regulate osteoblastogenesis through the inhibition of the NF-κB signaling pathway. On the basis of the conclusions of current and past research, which indicates that AP had both stimulating effects on osteoblastogenesis and inhibitory activity on osteoclastogenesis, along with its safety in clinical practice, it is reasonable and responsible to propose that AP has a great potential to be an ideal antiresorptive and

Figure 4 AP inhibits TNF-α—mediated suppression of osteoblast mineralization and downregulates TNF-α—mediated stimulation of the NF-κB signaling pathway. (A) Alizarin red S staining. (B) The number of calcified nodules. (C) Calcified nodule area. (D) mRNA expression of OCN, OPN and Runx2. (E) NF-κB luciferase activity up stimulation with the indicated AP, TNF-α and BMP-2. (F) Osteoblast-specific gene expression of OCN. Data are presented as mean ± SD; *P < 0.05. AP, andrographolide; NF-κB, nuclear factor kappa-B; OCN, osteocalcin; OPN, osteopontin; Runx2, runt-related transcription factor-2; TNF-α, tumor necrosis factor alpha; SD, standard deviation; BMP-2, bone morphogenetic protein-2.

osteoanabolic agent to inhibit bone resorption and promote the formation of bone simultaneously to stop oestrogen deficiency—induced bone loss.

Conflicts of interest

The authors have no conflicts of interest to declare.

Acknowledgements

This work was supported by the National Natural Science Foundation (Grant No. 81672181) and Shanghai JiaoTong University Medical and Engineering Cross Fund (Grant No. YG2017MS09).

Appendix A. Supplementary data

Supplementary data related to this article can be found at https://doi.org/10.1016/j.jot.2019.02.001.

References

[1] Khosla S, Hofbauer LC. Osteoporosis treatment: recent developments and ongoing challenges. Lancet Diabetes Endocrinol 2017;5(11):898—907.
[2] Keaveny TM, McClung MR, Genant HK, Zanchetta JR, Kendler D, Brown JP, et al. Femoral and vertebral strength improvements in postmenopausal women with osteoporosis treated with denosumab. J Bone Miner Res 2014;29(1):158—65.
[3] Guanabens N, Monegal A, Cerda D, Muxi A, Gifre L, Peris P, et al. Randomized trial comparing monthly ibandronate and weekly alendronate for osteoporosis in patients with primary biliary cirrhosis. Hepatology 2013;58(6):2070—8.
[4] Papapoulos SE. Bone diseases: bisphosphonates in osteoporosis-beyond 5 years. Nat Rev Rheumatol 2013;9(5):263—4.
[5] Amugongo SK, Yao W, Jia J, Lay YAE, Dai W, Jiang L, et al. Effects of sequential osteoporosis treatments on trabecular bone in adult rats with low bone mass. Osteoporos Int 2014;25(6):1735—50.
[6] Altman AR, Tseng WJ, de Bakker CMJ, Huh BK, Chandra A, Qin L, et al. A closer look at the immediate trabecula response to combined parathyroid hormone and alendronate treatment. Bone 2014;61:149—57.
[7] Cosman F, Eriksen EF, Recknor C, Miller PD, Guanabens N, Kasperk C, et al. Effects of intravenous zoledronic acid plus subcutaneous teriparatide [rhPTH(1-34)] in postmenopausal osteoporosis. J Bone Miner Res 2011;26(3):503—11.
[8] Cusano NE, Bilezikian JP. Combination antiresorptive and osteoanabolic therapy for osteoporosis: we are not there yet. Curr Med Res Opin 2011;27(9):1705—7.
[9] Finkelstein JS, Wyland JJ, Lee H, Neer RM. Effects of teriparatide, alendronate, or both in women with postmenopausal osteoporosis. J Clin Endocrinol Metab 2010;95(4):1838—45.
[10] McClung MR, Grauer A, Boonen S, Bolognese MA, Brown JP, Diez-Perez A, et al. Romosozumab in postmenopausal women with low bone mineral density. N Engl J Med 2014;370(5):412—20.
[11] Saag KG, Petersen J, Brandi ML, Karaplis AC, Lorentzon M, Thomas T, et al. Romosozumab or alendronate for fracture prevention in women with osteoporosis. N Engl J Med 2017;377(15):1417—27.
[12] An J, Yang H, Zhang Q, Liu C, Zhao J, Zhang L, et al. Natural products for treatment of osteoporosis: the effects and mechanisms on promoting osteoblast-mediated bone formation. Life Sci 2016;147:46—58.
[13] An J, Hao D, Zhang Q, Chen B, Zhang R, Wang Y, et al. Natural products for treatment of bone erosive diseases: the effects and mechanisms on inhibiting osteoclastogenesis and bone resorption. Int Immunopharmacol 2016;36:118—31.
[14] Che CT, Wong MS, Lam CW. Natural products from Chinese medicines with potential benefits to bone health. Molecules 2016;21(3):239.
[15] Edwin ES, Vasantha-Srinivasan P, Senthil-Nathan S, Thanigaivel A, Ponsankar A, Pradeepa V, et al. Anti-dengue efficacy of bioactive andrographolide from Andrographis paniculata (Lamiales: Acanthaceae) against the primary dengue vector Aedes aegypti (Diptera: Culicidae). Acta Trop 2016;163:167—78.
[16] Tan WSD, Liao WP, Zhou S, Wong WSF. Is there a future for andrographolide to be an anti-inflammatory drug? Deciphering its major mechanisms of action. Biochem Pharmacol 2017;139:71—81.
[17] Wen L, Xia N, Chen XH, Li YX, Hong Y, Liu YJ, et al. Activity of antibacterial, antiviral, anti-inflammatory in compounds andrographolide salt. Eur J Pharmacol 2014;740:421—7.
[18] Zhao J, Yang G, Liu H, Wang D, Song X, Chen Y. Determination of andrographolide, deoxyandrographolide and neoandrographolide in the Chinese herb Andrographis paniculata by micellar electrokinetic capillary chromatography. Phytochem Anal 2002;13(4):222—7.
[19] Ji X, Li C, Ou Y, Li N, Yuan K, Yang G, et al. Andrographolide ameliorates diabetic nephropathy by attenuating hyperglycemia-mediated renal oxidative stress and inflammation via Akt/NF-kappaB pathway. Mol Cell Endocrinol 2016;437:268—79.
[20] Ding Y, Chen L, Wu W, Yang J, Yang Z, Liu S. Andrographolide inhibits influenza A virus-induced inflammation in a murine model through NF-kappaB and JAK-STAT signaling pathway. Microb Infect 2017;19(12):605—15.
[21] Peng T, Hu M, Wu TT, Zhang C, Chen Z, Huang S, et al. Andrographolide suppresses proliferation of nasopharyngeal carcinoma cells via attenuating NF-kappaB pathway. BioMed Res Int 2015;2015:735056.
[22] Zhang M, Xue E, Shao W. Andrographolide promotes vincristine-induced SK-NEP-1 tumor cell death via PI3K-AKT-p53 signaling pathway. Drug Des Dev Ther 2016;10:3143—52.
[23] Lin L, Li R, Cai M, Huang J, Huang W, Guo Y, et al. Andrographolide ameliorates liver fibrosis in mice: involvement of TLR4/NF-kappaB and TGF-beta1/smad2 signaling pathways. Oxid Med Cell Longev 2018;2018:7808656.
[24] Wong SY, Tan MG, Banks WA, Wong WS, Wong PT, Lai MK. Andrographolide attenuates LPS-stimulated up-regulation of C-C and C-X-C motif chemokines in rodent cortex and primary astrocytes. J Neuroinflammation 2016;13:34.
[25] Chen HW, Huang CS, Li CC, Lin AH, Huang YJ, Wang TS, et al. Bioavailability of andrographolide and protection against carbon tetrachloride-induced oxidative damage in rats. Toxicol Appl Pharmacol 2014;280(1):1—9.
[26] Chen HW, Huang CS, Liu PF, Li CC, Chen CT, Liu CT, et al. Andrographis paniculata extract and andrographolide modulate the hepatic drug metabolism system and plasma tolbutamide concentrations in rats. Evid Based Complement Altern Med 2013;2013:982689.
[27] Wedemeyer C, Xu J, Neuerburg C, Landgraeber S, Malyar NM, von Knoch F, et al. Particle-induced osteolysis in three-dimensional micro-computed tomography. Calcif Tissue Int 2007;81(5):394—402.
[28] Houlihan DD, Mabuchi Y, Morikawa S, Niibe K, Araki D, Suzuki S, et al. Isolation of mouse mesenchymal stem cells on

the basis of expression of Sca-1 and PDGFR-α. Nat Protoc 2012;7(12):2103.
[29] Chang J, Wang Z, Tang E, Fan Z, McCauley L, Franceschi R, et al. Inhibition of osteoblast functions by IKK/NF-κB in osteoporosis. Nat Med 2009;15(6):682.
[30] Jimi E, Hirata S, Shin M, Yamazaki M, Fukushima H. Molecular mechanisms of BMP-induced bone formation: cross-talk between BMP and NF-κB signaling pathways in osteoblastogenesis. Jpn Dent Sci Rev 2010;46(1):33—42.
[31] Eliseev RA, Schwarz EM, Zuscik MJ, O'Keefe RJ, Drissi H, Rosier RN. Smad7 mediates inhibition of Saos2 osteosarcoma cell differentiation by NFκB. Exp Cell Res 2006;312(1):40—50.
[32] Gilbert LC, Rubin J, Nanes MS. The p55 TNF receptor mediates TNF inhibition of osteoblast differentiation independently of apoptosis. Am J Physiol Endocrinol Metab 2005;288(5): E1011—8.
[33] Li Y, Li A, Strait K, Zhang H, Nanes MS, Weitzmann MN. Endogenous TNFα lowers maximum peak bone mass and inhibits osteoblastic Smad activation through NF-κB. J Bone Miner Res 2007;22(5):646—55.
[34] Chang J, Liu F, Lee M, Wu B, Ting K, Zara JN, et al. NF-kappaB inhibits osteogenic differentiation of mesenchymal stem cells by promoting beta-catenin degradation. Proc Natl Acad Sci U S A 2013;110(23):9469—74.
[35] Lin TH, Gibon E, Loi F, Pajarinen J, Cordova LA, Nabeshima A, et al. Decreased osteogenesis in mesenchymal stem cells derived from the aged mouse is associated with enhanced NF-kappaB activity. J Orthop Res 2017;35(2):281—8.
[36] Wang T, Li S, Yi D, Zhou GQ, Chang Z, Ma PX, et al. CHIP regulates bone mass by targeting multiple TRAF family members in bone marrow stromal cells. Bone Res 2018;6:10.